

Theoretical studies of plasmon resonances in one-dimensional nanoparticle chains: narrow lineshapes with tunable widths

This article has been downloaded from IOPscience. Please scroll down to see the full text article.

2006 Nanotechnology 17 2813

(<http://iopscience.iop.org/0957-4484/17/11/014>)

View [the table of contents for this issue](#), or go to the [journal homepage](#) for more

Download details:

IP Address: 162.105.246.83

The article was downloaded on 17/05/2011 at 06:01

Please note that [terms and conditions apply](#).

Theoretical studies of plasmon resonances in one-dimensional nanoparticle chains: narrow lineshapes with tunable widths

Shengli Zou and George C Schatz

Department of Chemistry, Northwestern University, 2145 Sheridan Road, Evanston, IL 60208-3113, USA

Received 23 December 2005

Published 22 May 2006

Online at stacks.iop.org/Nano/17/2813

Abstract

In this paper we describe a new configuration for producing narrow extinction lineshapes for light scattering from one-dimensional arrays of silver nanoparticles. In this configuration, which is specifically concerned with an array with a finite number of relatively large (radius greater than around 30 nm) nanoparticles, the wavevector of the light is chosen to be parallel to the array axis, while the polarization direction is perpendicular to the array axis. This leads to narrow plasmon/photonic lineshapes when the particle spacing is *half* the incident wavelength. This effect stands in contrast to the narrow lines previously found for wavevector and polarization vector perpendicular to the array axis, where the optimum spacing is close to the wavelength. The results are rationalized using a semi-analytical evaluation of the coupled dipole interaction, and it is demonstrated that the parallel and perpendicular chains have very different dependence on the number of particles in the chain. Results as a function of chain orientation relative to the wavevector are also considered, as is the possibility of sensing using an array configuration that combines the parallel and perpendicular chain directions.

(Some figures in this article are in colour only in the electronic version)

1. Introduction

The unique optical properties of noble metal nanoparticles have stimulated intense scientific research in such fields as medical diagnostics and optoelectronics [1–7]. For a single metal nanoparticle, the plasmon resonance, which is a collective excitation of the conduction electrons, depends on its composition, size, shape, and surrounding medium, and this provides important functionality for controlling such optical properties as extinction and scattering to signal the presence of adsorbed molecules, and to manipulate pulses of light [8, 9]. In arrays of nanoparticles, the electromagnetic couplings between particles induces photonic effects that can interact with plasmon excitation in each particle to alter the plasmon lineshape in ways that depend on particle spacings and polarization and wavevector directions [10–17]. If the particle spacings are small compared to the plasmon wavelength, then this typically produces red-shifted plasmon bands in extinction spectra, although blue-shifted bands can result for some choices of particle geometry and polarization.

Somewhat larger spacings (100–200 nm) can lead to important retardation (e^{ikr}) and radiative ($1/r$) contributions to the dipolar interactions between particles that can convert red-shifted plasmon lineshapes into blue-shifts [10]. The present paper is concerned with what happens for still larger spacings, of the order of 0.5–1.0 times the plasmon wavelength (250–500 nm for silver), where diffractive interactions between the particles are important, leading to new structures (both maxima and minima) in extinction spectra.

In previous papers, we used a simple theoretical method known as the coupled dipole approximation to study the plasmon resonance lineshapes associated with light scattering from one- and two-dimensional silver nanoparticle arrays [12, 13]. Narrow peaks (<10 nm) in the extinction spectra were found for the case where the array spacing is somewhat larger than the isolated particle plasmon wavelength and slightly smaller than the wavelength of light. It was also found that significant peaks only occur when the particles are larger than a minimum value (sphere radius greater than

30 nm), and that the peaks are often accompanied by dips to the blue of the peaks. This structure is related to results obtained from earlier studies of surface enhanced Raman scattering from square two-dimensional arrays by Carron *et al* [11] and the influence of dipolar interactions on the plasmon in two-dimensional Au nanoparticles by Aussenegg's group [16, 17], but we found that the narrowest plasmon resonances occur for one-dimensional chains. There is also an important connection between these results and the peaks and dips that are seen in the transmission spectra of nanohole arrays [18–21].

Our earlier results considered chains where the array axis is perpendicular to the wavevector and polarization directions. In this case, a peak in the extinction spectrum with width less than 1 nm was calculated [12]. A semi-analytical formula was used to investigate the mechanism [22], following up Markel's earlier work [23, 24], and this demonstrated that the narrow peaks are primarily determined by the strong wavelength dependence of the sum of dipolar interactions. The dispersion properties of these chain structures were also discussed by Citrin [25]. By optimizing the particle size and interparticle distance, it was recently discovered that one-dimensional chains are very efficient in waveguide applications [26].

The induced electric fields near the particle surfaces were also examined for these array structures [27], and it was found that the dipolar interactions also produce large field enhancements, leading to the possibility of larger SERS enhancements than can be obtained for isolated particles or small clusters of particles. However surface enhanced Raman scattering applications based on these array structures are constrained by the requirement that the field be enhanced at both incident and Stokes shifted wavelengths, which is difficult to achieve with a chain of nanoparticles having a single spacing.

Recent experiments carried out by Hicks *et al* [14] have at least partially confirmed theoretical predictions concerning the plasmon lineshapes of one-dimensional silver particle chains [12, 13]. In the experiments, one-dimensional chains of silver discs separated by two microns were fabricated by e-beam lithography [28]. Rayleigh scattering spectra for these arrays revealed an extra peak that tunes with array spacing in a fashion that is consistent with the expectations of theory, although the width of this photonic peak was broader in the measurements. Similar behaviour was also noted by Lamprecht *et al* [16] for two-dimensional arrays. The difference in width is likely due to the use of an incoherent light source in the experiments, along with dephasing due to the incident light that was not normal to the chain axis, and indeed models that included these factors were in better agreement with the measurements [14]. Two other factors which were found to be crucial in producing the narrow peak are homogeneity of the surrounding medium (i.e., index matching fluids were used in the Hicks *et al* work, but not in the other studies cited) and large particle size. If the particle arrays are on a substrate, the dipolar interactions between the particles are partially dephased, and a narrow lineshape is not produced. Also, for small particles, the dipolar interactions are too weak to produce observable diffractive coupling. Further confirmation of these results has recently been provided [29, 30].

In the present paper, we report another approach for producing narrow plasmon resonance peaks using chains of

nanoparticles. In this version, the wave vector is taken to be parallel (rather than perpendicular) to the chain axis, leading to an optimal particle spacing that is about half of the wavelength of light (i.e., half the spacing of our earlier array structure). There are also important differences in the dependence of the results on array size, and additional resonances where the wavelength equals the array spacing are found. By combining arrays for the parallel and perpendicular cases, we demonstrate a new structure for optical sensing applications that is superior for single particle or SERS studies to that which we have considered previously.

2. Methods

We use T -matrix theory [31, 32], the coupled dipole (CD) approximation [33] and a semi-analytical formula based on CD to investigate the extinction spectra of one-dimensional particle arrays. When the particles are well separated, the CD method provides a quantitative description of the optical properties of the array. The T -matrix theory that we use includes higher multipole interactions, and as such it provides an efficient method for modelling the electrodynamics of spherical particles with arbitrary radii and separations, enabling us to check the accuracy of the CD results when the particle separations are small.

In the coupled dipole method, we consider an array of N particles whose positions and polarizabilities are denoted \mathbf{r}_i and α_i . The induced polarization \mathbf{P}_i in each particle in the presence of an applied plane wave field is $\mathbf{P}_i = \alpha_i \mathbf{E}_{\text{loc},i}$ ($i = 1, 2, \dots, N$) where the local field $\mathbf{E}_{\text{loc},i}$ is the sum of the incident and retarded fields of the other $N - 1$ dipoles. For a given wavelength λ , this field is:

$$\mathbf{E}_{\text{loc},i} = \mathbf{E}_{\text{inc},i} + \mathbf{E}_{\text{dipole},i} = E_0 \exp(i\mathbf{k} \cdot \mathbf{r}_i) - \sum_{\substack{j=1 \\ j \neq i}}^N \mathbf{A}_{ij} \cdot \mathbf{P}_j \quad i = 1, 2, \dots, N, \quad (1)$$

where E_0 and $k = 2\pi/\lambda$ are the amplitude and wavevector of the incident wave, respectively. The dipole interaction matrix \mathbf{A} is expressed as:

$$\begin{aligned} \mathbf{A}_{ij} \cdot \mathbf{P}_j &= k^2 e^{ikr_{ij}} \frac{\mathbf{r}_{ij} \times (\mathbf{r}_{ij} \times \mathbf{P}_j)}{r_{ij}^3} \\ &+ e^{ikr_{ij}} (1 - ikr_{ij}) \frac{[r_{ij}^2 \mathbf{P}_j - 3\mathbf{r}_{ij}(\mathbf{r}_{ij} \cdot \mathbf{P}_j)]}{r_{ij}^5}, \end{aligned} \quad (i = 1, 2, \dots, N, j = 1, 2, \dots, N, j \neq i), \quad (2)$$

where \mathbf{r}_{ij} is the vector from dipole i to dipole j .

Note that the first term in equation (2) has a $1/r$ dependence on interparticle spacing, while the second has $1/r^2$ and $1/r^3$ variations. As a result, the first term, which is associated with radiative dipolar interactions between the particles, is often dominant for large array spacings.

The polarization vectors are obtained by solving $3N$ linear equations of the form

$$\tilde{\mathbf{A}}' \mathbf{P} = \mathbf{E}, \quad (3)$$

where the off diagonal elements of the matrix $\tilde{\mathbf{A}}'$, \mathbf{A}'_{ij} are the same as \mathbf{A}_{ij} , and the diagonal elements, \mathbf{A}'_{ii} , are α_i^{-1} .

After obtaining the polarization vectors, we can calculate the extinction cross section using:

$$C_{\text{ext}} = \frac{4\pi k}{|E_0|^2} \sum_{j=1}^N \text{Im}(E_{\text{inc},j}^* \cdot P_j). \quad (4)$$

A simple analytical solution [33] to (3) can be obtained in the case of an infinite array of particles for the case where the wavevector is perpendicular to the array axis (or plane) by assuming that the induced polarization in each array element is the same. This leads to the following expression for the polarization of each particle:

$$P = \frac{\alpha_s E_0}{1 - \alpha_s S} = \frac{E_0}{1/\alpha_s - S} \quad (5)$$

and the extinction cross section for each particle

$$C_{\text{ext}} = 4\pi k \text{Im} \left(\frac{P}{E_0} \right) = 4\pi k \text{Im} \left(\frac{1}{1/\alpha_s - S} \right), \quad (6)$$

where S is the retarded dipole sum

$$S = \sum_{j \neq i} \left[\frac{(1 - ikr_{ij})(3 \cos^2 \theta_{ij} - 1)e^{ikr_{ij}}}{r_{ij}^3} + \frac{k^2 \sin^2 \theta_{ij} e^{ikr_{ij}}}{r_{ij}} \right]. \quad (7)$$

The polarizability in equation (6) is

$$\alpha_s = \frac{3a_1}{2k^3} \quad (8)$$

where k is the wavevector of the incident wave, and a_1 is the expansion coefficient in Mie theory associated with the scattered electric fields around the particles. This is given by

$$a_1 = \frac{\mu m^2 j_1(m\rho)[\rho j_1(\rho)]' - \mu_1 j_1(\rho)[m\rho j_1(m\rho)]'}{\mu m^2 j_1(m\rho)[\rho h_1^1(\rho)]' - \mu_1 h_1^1(\rho)[m\rho j_1(m\rho)]'}. \quad (9)$$

In this expression, $\rho = kr$, where r is the radius of the particle, m is the ratio of the indices of refraction inside and outside the particle, μ_i , μ_o are the magnetic permeabilities inside and outside, and j_1 , h_1 are the usual spherical Bessel functions. Note that because the polarizabilities are taken from Mie theory, radiative damping and depolarization effects are included that broaden the resonances for large particles. These broadening effects are partially cancelled by the radiative dipolar interactions, which is one of the reasons why narrow lineshapes can be produced by particle arrays [22]. Indeed, in our earlier work, we used equation (5) to show how coupling between the particles leads to a sharp peak in the plasmon resonance lineshape [12, 13, 33].

Now let us generalize this derivation to consider a general three-dimensional periodic array. Here equation (5) still applies, but the dipole sum is modulated by an extra term e^{ikz} (where z measures the distance along the wavevector). If we take the polarization to be in the X direction, then equation (7) is replaced by:

$$S = \sum_{j \neq i} e^{ikz_j} \left[\frac{(1 - ikr_{ij})(3x_{ij}^2 - r_{ij}^2)e^{ikr_{ij}}}{r_{ij}^5} + \frac{k^2(y_{ij}^2 + z_{ij}^2)e^{ikr_{ij}}}{r_{ij}^3} \right] = \sum_{j \neq i} e^{ik(r_{ij}z_j)} \times \left[\frac{(1 - ikr_{ij})(3x_{ij}^2 - r_{ij}^2)}{r_{ij}^5} + \frac{k^2(y_{ij}^2 + z_{ij}^2)}{r_{ij}^3} \right] \quad (10)$$

where z_{jj} is the Z axis coordinate of the particle j relative to the particle i , etc.

In equation (10), the first term in the square bracket corresponds to the short range dipole interaction. This leads to strong interactions between particles for the case where the array is a chain along the polarization direction [34, 35]. The second term represents the long range interaction. In this case, if the chain is parallel to the polarization direction (X axis), then the long range term is zero, and narrow lines are not produced [12]. The best structures for generating long range interactions are chains in the YZ plane, especially a one-dimensional chain along the Y axis which is what we considered previously [12]. For one-dimensional chains in the YZ plane, to have the in-phase interactions, we may easily derive from equation (10) that

$$k(r_{ij} + z_{ij}) = n2\pi \quad r_{ij} + z_{ij} = n\lambda. \quad (11)$$

Thus if θ is the angle between the chain and wavevector directions, the optimum spacing is:

$$r_{ij} = \frac{n\lambda}{1 + \cos \theta}. \quad (12)$$

This is same result that Carron *et al* [11] derived for two-dimensional square arrays, and it leads to $r = n\lambda$ when the chain is perpendicular to the k -vector direction (matching our earlier result [12, 13]), and $r = n\lambda/2$ for the parallel case. It is this latter case that we will examine in detail below.

3. Results and discussion

We first consider a one-dimensional chain of 50 nm radius spherical silver particles with different interparticle distances. 200 particles are included for the parallel case and 400 particles for the perpendicular arrangement, with the polarization vector in all calculations taken to be perpendicular to the chain axis. The dielectric constants of silver are from the handbook of Lynch *et al* [36].

The extinction spectra from T -matrix calculations are shown in figure 1 (top) for the case where the chain is parallel to the wavevector direction, and CD results are presented for the perpendicular case in figure 1 (bottom). (The CD and T -matrix results are identical with respect to the narrow peaks for the latter case, which refers to larger particle separations, as demonstrated previously [12].) For the perpendicular wavevector, a broad plasmon resonance is seen for small interparticle spacings (200 nm) that is blue-shifted from the isolated particle resonance (dotted curve) showing the effect of static dipolar interactions. This resonance red-shifts as the particle spacing is increased, and gradually splits into two peaks, a broad one at around 400 nm, and a narrow one at a wavelength that is slightly larger than the particle spacing. The most intense of the narrow resonances occurs at a spacing of 470 nm, a width of 3.5 nm and a maximum extinction efficiency of 22.

For the parallel case, the resonance is red-shifted from the isolated particle resonance for small interparticle spacings (110 nm), and then blue-shifts as the spacing is increased up to 200 nm. For larger spacings, the lineshape splits into two peaks, a broad one at around 450 nm, and a narrow one at

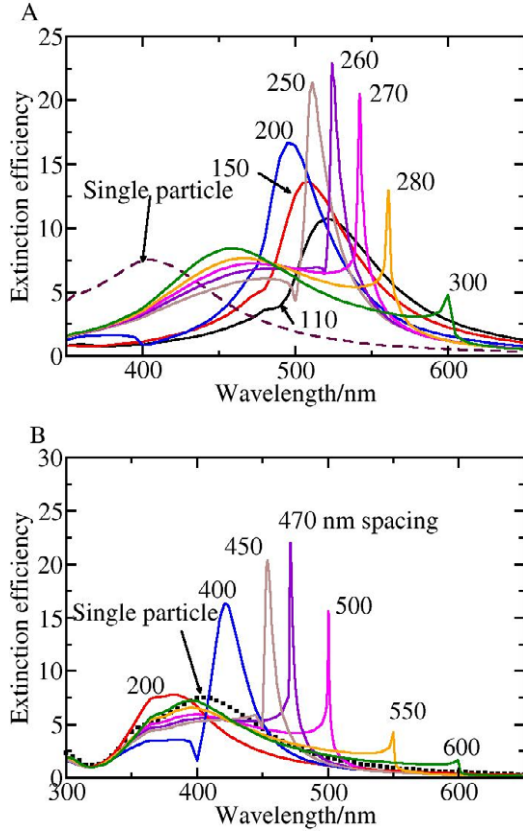


Figure 1. Extinction spectra of a one-dimensional chain of 50 nm silver particles with different interparticle distances and orientations. Top: parallel to the wavevector direction. Bottom: perpendicular to the wavevector direction.

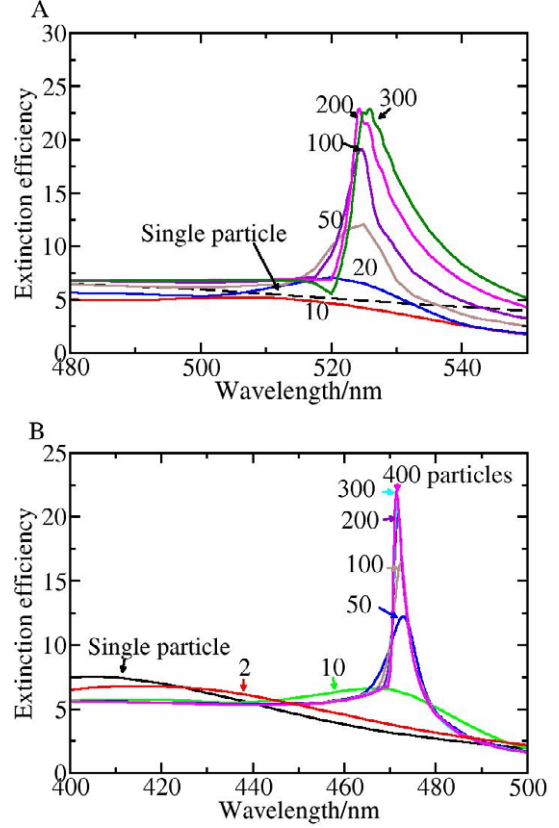


Figure 2. Extinction spectra of a one-dimensional chain of 50 nm particles. Top: chain parallel to the wavevector direction for a spacing of 260 nm with chain size varying from 10 to 300 particles. Bottom: chain perpendicular to the wavevector direction for a spacing of 470 nm with chain size varying from 2 to 400 particles.

a wavelength that is close to half the particle spacing. The highest intensity of resonance peaks occurs at 260 nm spacing. Here the resonance wavelength is at 524 nm, and the width of the resonance peak is 10 nm with an extinction efficiency of 23.

After examining the distance dependence of the spectra, we investigate the extinction spectra of a one-dimensional chain as a function of the number of particles in the chain. These results are presented in figure 2, with figure 2 (top) showing the parallel wavevector case for a spacing of 260 nm, and figure 2 (bottom) the perpendicular case for a spacing of 470 nm. The chain size varies from 2 to 300 particles. For both cases, it takes about 50 particles to generate a narrow resonance, but there are important differences in the variation of the results with particle number. Figure 2 (bottom) shows that convergence of resonance lineshape with increasing particle number is relatively fast for the perpendicular case, with very little change between 300 and 400 particles. Figure 2 (top) shows much slower convergence with particle number for the parallel case, and indeed the results are not close to being converged with 300 particles.

As long as the particle spacings are larger than around 200 nm, it is possible to use the CD method instead of T -matrix theory to model the narrow plasmon lineshapes with essentially no error in the results. This enables us to study the behaviour of the spectra for much larger particle numbers,

especially if we use the semi-analytical formula based on equations (5) and (10). Figure 3 presents extinction spectra based on this approach for arrays with 500 particles and a parallel wavevector. These results are analogous to those in figure 1 (top), however the number of particles is larger, so the results show quantitative differences. In particular, when the particle distances varies from 250 to 300 nm (compare figure 1 (top) and 3 (bottom)), the sharp peak is narrower and more intense for the larger particle number. Indeed, for a spacing of 290 nm, the peak occurs at 590 nm with an extinction efficiency of 24 and a width of 2 nm. Note also that for spacings of 300 nm and higher, a second sharp peak appears in figure 3 (top) at a wavelength that is about equal to the spacing (this is most noticeable for the 500 nm spacing). This is the $n = 2$ peak in the formula $r = n\lambda/2$ that we gave earlier, and we see that this peak is a dip when it occurs to the blue of the isolated plasmon wavelength and a peak when it occurs to the red. The origin of the switch from a dip to a peak is similar to that described in our earlier work [25] and it arises from a change in sign of the real part of the isolated particle polarizability as one tunes through the plasmon resonance peak at 470 nm.

In the following paragraphs, we discuss the convergence of the calculations based on equations (5) and (10) with respect to particle number for very large particle numbers, considering a one-dimensional chain parallel to the wavevector. Figure 4 presents results for spacings of 250 and 280 nm for particle

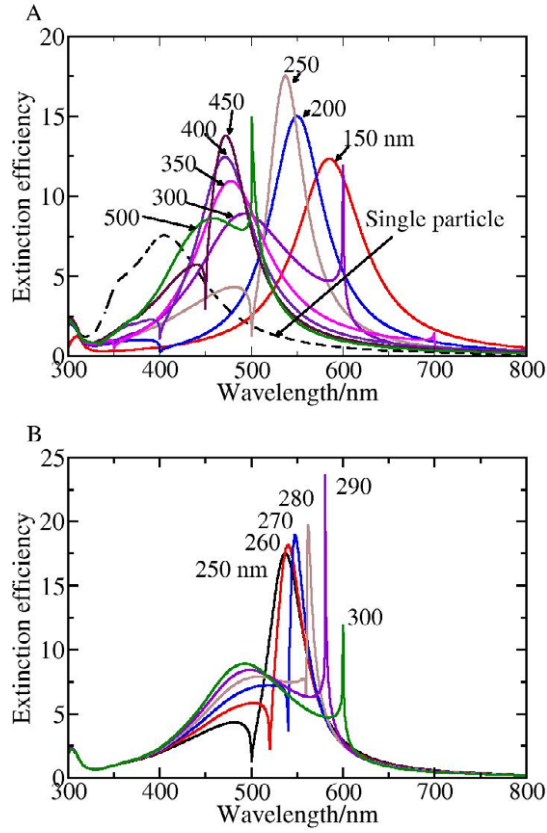


Figure 3. Extinction spectra of a one-dimensional chain of 50 nm particles (500 particles) parallel to the wavevector direction, with different spacings. This result is from the semi-analytical formula. Bottom plot highlights the 250–300 nm region.

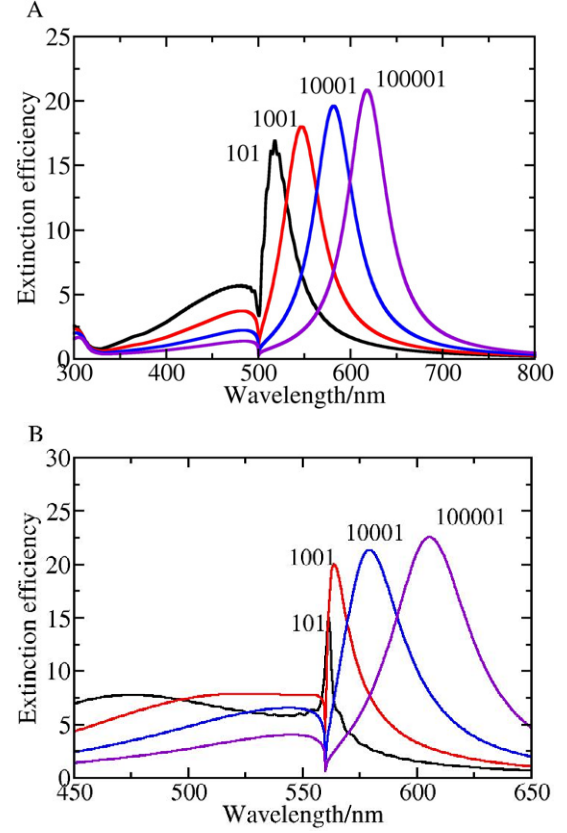


Figure 4. Extinction spectra of a one-dimensional chain of 50 nm particles with spacings of 250 nm (top) and 280 nm (bottom) based on the semi-analytical formula. The chain size varies from 101 to 100 001 particles.

numbers from 101 to 100 001. Figure 4 (top) shows results for a spacing of 250 nm, where there is a dip at roughly 500 nm wavelength. When 101 particles are included in the calculations, the resonance peak occurs at 518 nm with a width of 33 nm. The resonance wavelength red-shifts to 618 nm when 100 001 particles are included, and the width is increased to 52 nm. The corresponding peak intensity is increased from 17 to 21. Figure 4 (bottom) plots analogous results for a spacing of 280 nm. When 101 particles are included in the calculations, a peak with 3 nm width is found at 561 nm. As the particle number increases to 10001 particles, this narrow peak broadens (width = 43 nm) and red-shifts (to 605 nm). This surprising tunability of the plasmon resonance wavelength and width for very large particle numbers (arrays that are 6 mm in length) arises from the extremely long range of the dipole sum. Although it is unlikely that this would be of use in practical applications, we note that broad resonances like this allow for easier use of these structures in SERS studies, where enhancement at both incident and Stokes shifted wavelength can be achieved [27].

To understand the origin of the tunable width of the plasmon resonance with particle number for the parallel case, we examine the retarded dipole sum in equation (10). The real and imaginary parts of the dipole sum for the chain considered in figure 4 (bottom) with a spacing of 280 nm are presented as a function of particle number in figure 5.

This figure shows that the imaginary part of the dipole sum converges very quickly with particle number, while the real part grows linearly with the logarithm of the particle number. This behaviour is related to the conclusions of our earlier analysis [25], where we demonstrated for the perpendicular case that the real part of the dipole sum would diverge logarithmically at the resonance wavelength, however here we see that the logarithmic divergence occurs over a wide range of wavelengths for the parallel case. This arises because the exponent $ik(r_{ij} + z_j)$ in equation (10) vanishes whenever $z = -r_{ij}$, which happens for all the particles j in the array which are ‘in-front’ of particle i . When this exponent vanishes, the terms in the dipole sum add constructively, independent of wavelength. Physically this arises because the phase of the plane wave field at particle i is the same as that of the retarded dipole interaction arising from any particle j that is in front of i .

To understand how the results in figure 5 determine the behaviour in figure 4 (bottom), in figures 6 and 7 we compare the imaginary and real parts, respectively, of the dipole sum with the inverse polarizability $1/\alpha$ that appears in the denominator in equation (5). In order for the induced polarization P in equation (5) to become large, it is necessary for both the imaginary and real parts of the denominator to be small or zero at the same wavelength.

Figure 7 shows that there is a sudden step in the imaginary part of the dipole sum at about 560 nm which makes this sum

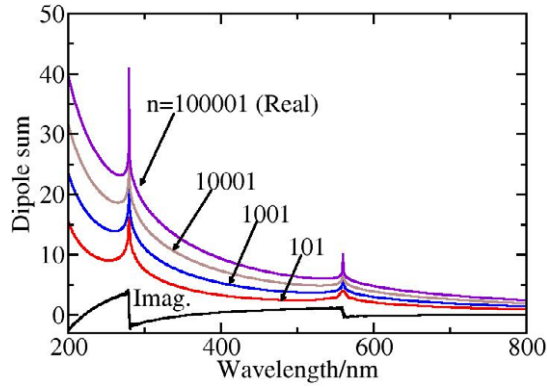


Figure 5. Real and imaginary parts of the dipole sum for a chain parallel to the wavevector direction with a spacing of 280 nm, and particle numbers varying from 101 to 100 001.

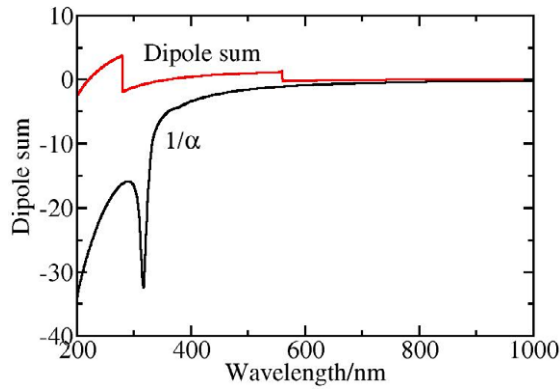


Figure 6. Imaginary part of the dipole sum for a chain parallel to the wavevector direction with a spacing of 280 nm. The imaginary part of the reciprocal of the polarizability for a single particle is also plotted.

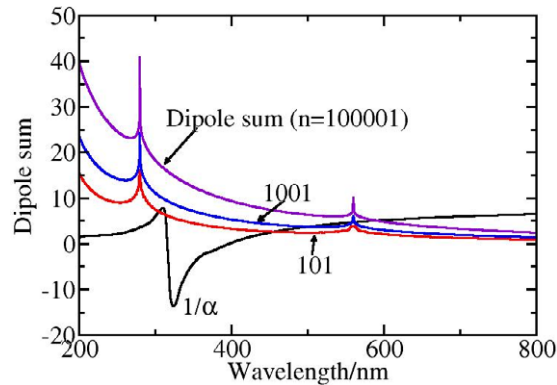


Figure 7. Real part of the dipole sum for a chain parallel to the wavevector direction with a spacing of 280 nm. The real part of the reciprocal of the polarizability is also plotted.

very close in value to $1/\alpha$ at longer wavelengths. Thus it is not surprising that there can be a sharp peak or dip in figure 4 (bottom) at a wavelength slightly longer than this, however the sharp structure is due to the real part of the dipole sum. Figure 7 shows that the real part of the dipole sum has a sharp

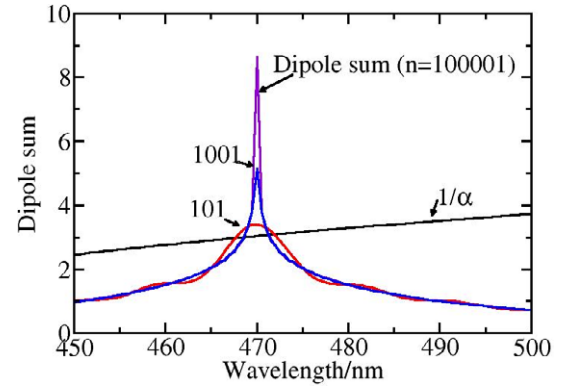


Figure 8. Real part of the dipole sum for a chain perpendicular to the wavevector direction with a spacing of 470 nm. The reciprocal of the polarizability for a single particle is also plotted.

peak at 560 nm which crosses the real part of $1/\alpha$ near 560 nm for the 101 particle case, but not for the 100 001 particle case. For the 101 particle case, this leads to a sharp peak, since the real and imaginary parts of the denominator in equation (5) are small at the same time. However for the 100 001 particle case, the real part of the denominator grows larger in magnitude as one tunes through the peak, and this leads to a dip rather than a peak.

Examination of figures 6 and 7 also provides an explanation for other features in figure 4. For example, there is a ‘valley’ in the $1/\alpha$ term in figure 6 at 310 nm wavelength that arises from interband transitions in silver. This valley produces the minimum at that same wavelength in figure 4 (top). Figure 7 shows a maximum in the dipole sum at 280 nm as well as the one at 560 nm that we discussed above. The 280 nm peak also produces a sharp structure in extinction spectra (not shown in figure 4), but since there is no intersection between the dipole sum and $1/\alpha$ at this wavelength, the sharp structure is a dip rather than a peak.

Another feature arises from the crossing at 470 nm in figure 7 between the $1/\alpha$ curve and the dipole sum with 101 particles. This crossing leads to a peak at that wavelength in figure 4 (bottom), but because it is a crossing of two relatively flat curves, the peak is broad. Also, since the crossing occurs at a point where the imaginary terms in figure 6 are well separated, the intensity at this wavelength is relatively low. A similar crossing occurs between the 100 001 particle curve at $1/\alpha$ in figure 7 at 620 nm. This leads to the peak at 620 nm in figure 4 (bottom), but again note that it is relatively broad due to the fact that the curves in figure 7 are relatively flat where they cross. Moreover, we see in figure 7 that as the number of particles increases, the crossing with the $1/\alpha$ curve gradually red-shifts. This is the origin of the tunability of the long wavelength peak in figure 4, and it shows that in the limit of an infinite chain of particles, the resonance will shift to infinite wavelength. This also explains why the width of this peak gradually increases as particle number increases.

To complete this analysis, we show a plot similar to figure 7, but for the case where the wavevector is perpendicular to the chain axis. This is presented in figure 8 for a chain with a spacing of 470 nm, for wavelengths close to where the sharp peak in figures 1 (bottom) and 2 (bottom) occurs at

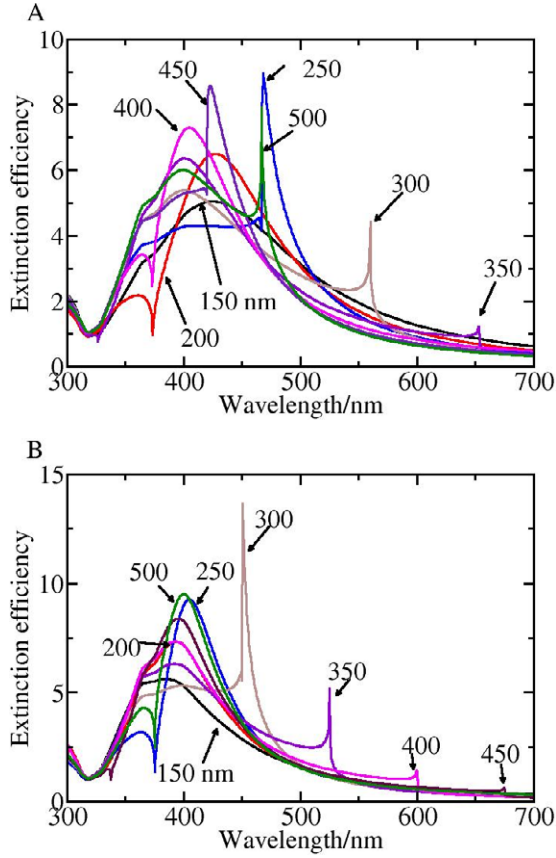


Figure 9. Extinction spectra of a chain with angles 30° (top) and 60° (bottom) from the wavevector direction.

470 nm. Only the real part of the terms in the denominator of equation (5) are included in the plot, as the imaginary part is analogous to that in figure 6 except that the drop of the imaginary part of the dipole sum at 560 nm occurs at 470 nm instead. We see in figure 8 that the two curves cross twice near 470 nm, and that the results for different particle numbers are much more similar than they are in figure 7. The crossing just below 470 nm does not lead to a sharp peak because the difference in imaginary terms is still large at that point, but the crossing just above 470 occurs at a point where the difference in imaginary terms is small, so this gives the sharp peak. This provides a simple way to visualize results that were previously explained in [14].

To further explore the predictions of equation (12), we now consider extinction spectra of one-dimensional chains that are oriented at different angles relative to the wavevector direction. These results are presented in figure 9, and we see that the narrow peaks closely follows the rule $r_{ij} = \frac{n\lambda}{1+\cos\theta}$.

One array structure that one could be of interest to sensing applications that follows from the analysis we have presented is a ‘+’ shaped array in which resonances associated with both parallel and perpendicular wavevectors are tuned to the same wavelength. There are many possible ways to do this, such as having the spacing in one direction be about half that in the other direction, however one especially interesting choice involves taking the two array spacings to be identical. Figure 10 presents extinction spectra for this structure, here

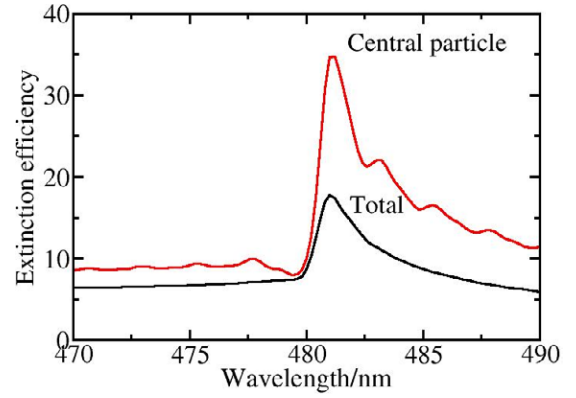


Figure 10. Extinction efficiency of the ‘+’ array configuration, along with the contribution to this extinction associated with the central particle in the structure.

considering arrays with 400 particles (so that the total number of particles is 799), with each particle being a 50 nm silver sphere, and a spacing of 480 nm. The contribution to the extinction spectrum from just the central particle in the structure is also plotted.

The results in figure 10 show a sharp resonance at 481 nm with a width of 2 nm. Significantly, the contribution of the central particle in the array to the extinction is about double that of the overall efficiency. This means that this particle represents a ‘hot spot’ in the array, with very large polarization, and a very strong effect on optical properties if the resonance wavelength of this particle is shifted as a result of adsorption of molecules on the particle. Electric field contour plots in the XZ plane through the centre of the central particle and the particle next to it (along the Y axis) are shown in figure 11. Figure 11 shows that the peak intensity ($|E|^2$) of the electric fields near the central particle is 1600, whereas the value is 780 for the particle near it. In earlier work [11], a one-dimensional chain of 50 nm silver particles (for perpendicular wavevector) was found to have a maximum $|E|^2$ of 700, so we see that the field associated with the central particle is more than a factor of two larger than was obtained with a single chain. Furthermore, this extra enhancement occurs for just one particle in the structure, so measurements associated with just that particle would be interesting, including the variation of the scattered light from that particle due to adsorbed molecules, and SERS measurements for that particle.

4. Conclusions

In this paper we have described the extinction spectra of one-dimensional chains of spherical nanoparticles under a variety of conditions that lead to the formation of sharp peaks in the extinction (and also scattering) spectra. Although the case of chains perpendicular to the wavevector was studied in some depth in earlier work, the parallel case was not considered, and our analysis was in fact generalized to describe chains making an arbitrary angle with the wavevector. We find that the parallel case leads to two important properties of the plasmon lineshape: the appearance of sharp peaks at roughly twice the particle spacing, and also at the particle spacing, and the tunability of peak wavelengths for very large particle numbers

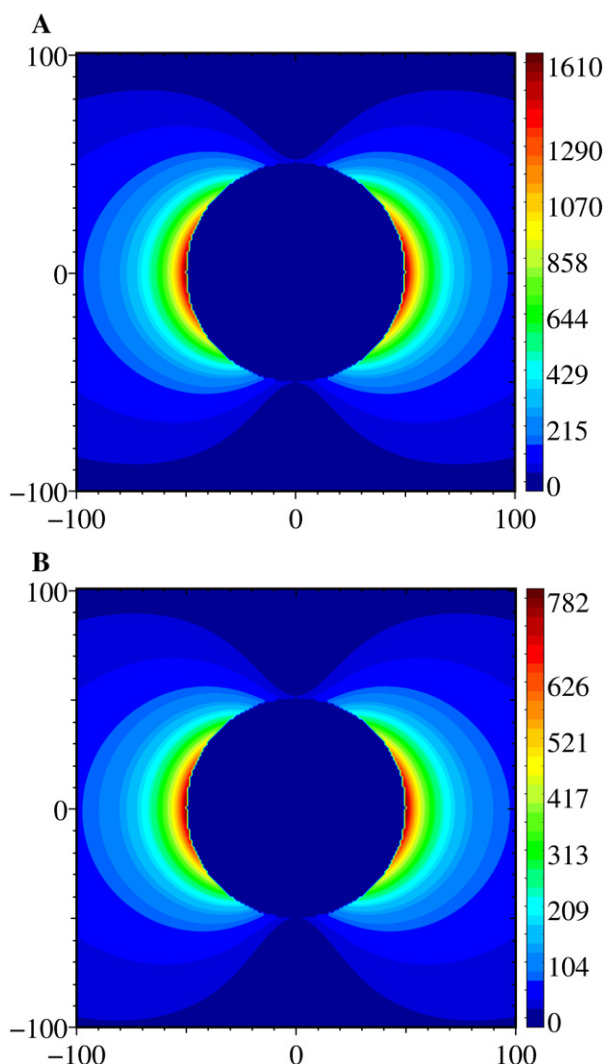


Figure 11. Electric field contour plot for particles of the '+' array configuration. Top: results for the central particle. Bottom: results for the particle next to the central particle.

(10^5). We examined the mechanism of these results, and we demonstrated the usefulness of plots that examine the real and imaginary parts of the dipole sum. Only when both the real and imaginary parts of the dipole sums are close the corresponding component of the reciprocal of the polarizability, can a narrow resonance peak occur. Finally we demonstrated how to use a combination of parallel and perpendicular clusters structures to combine the photonic resonances, leading to larger induced polarization, with potential applications in sensing.

Acknowledgments

This work was supported by the National Science Foundation through the Northwestern Materials Research Center, and by the Air Force Office of Scientific Research MURI program (F49620-02-1-0381).

References

- [1] Mirkin C A, Letsinger R L, Mucic R C and Storhoff J J 1996 *Nature* **382** 607
- [2] Boal A K, Ilhan F, DeRoucher J E, Thurn-Albrecht T and Rotello V M 2000 *Nature* **404** 746
- [3] Storhoff J J, Elghanian R, Mucic R C, Mirkin C A and Letsinger R L 1998 *J. Am. Chem. Soc.* **120** 1959
- [4] Elghanian R, Storhoff J J, Mucic R C, Letsinger R L and Mirkin C A 1997 *Science* **277** 1078
- [5] Van Duyne R P, Hulstee J C and Treichel D A 1993 *J. Chem. Phys.* **99** 2101
- [6] Maier S A, Kik P G, Atwater H A, Meltzer S, Harel E, Koel B E and Requicha A A G 2003 *Nat. Mater.* **2** 229
- [7] Maier S A, Kik P G and Atwater H A 2002 *Appl. Phys. Lett.* **81** 1714
- [8] Haynes C L and Van Duyne R P 2001 *J. Phys. Chem. B* **105** 5599
- [9] Kelly K L, Coronado E, Zhao L and Schatz G C 2003 *J. Phys. Chem. B* **107** 668
- [10] Haynes C L, McFarland A D, Zhao L, Van Duyne R P, Schatz G C, Gunnarsson L, Prikulis J, Kasemo B and Kall M 2003 *J. Phys. Chem. B* **107** 7337
- [11] Carron K T, Fluhr W, Meier M, Wokaun A and Lehmann H W 1986 *J. Opt. Soc. Am. B* **3** 430
- [12] Zou S, Janel N and Schatz G C 2004 *J. Chem. Phys.* **120** 10871
- [13] Zou S and Schatz G C 2004 *J. Chem. Phys.* **121** 12606
- [14] Hicks E M, Zou S, Schatz G C, Spears K G, Van Duyne R P, Gunnarsson L T R, Kasemo B and Kall M 2005 *Nano Lett.* **5** 1065
- [15] Zou S and Schatz G C 2004 *SPIE Proc.* **5513** 22
- [16] Lamprecht B, Schider G, Lechner R T, Ditlbacher H, Krenn J R, Leitner A and Aussenegg F R 2000 *Phys. Rev. Lett.* **84** 4721
- [17] Felidj N, Laurent G, Aubard J, Levi G, Hohenau A, Krenn J R and Aussenegg F R 2005 *J. Chem. Phys.* **123** 221103
- [18] Chang S-H, Gray S K and Schatz G C 2005 *Opt. Express* **13** 3150
- [19] Martin-Moreno L, Garcia-Vidal F J, Lezec H J, Pellerin K M, Thio T, Pendry J B and Ebbesen T W 2001 *Phys. Rev. Lett.* **86** 1114
- [20] Popov E, Neviere M, Enoch S and Reinisch R 2000 *Phys. Rev. B* **62** 16100
- [21] Ebbesen T W, Lezec H J, Ghaemi H F, Thio T and Wolff P A 1998 *Nature* **391** 667
- [22] Zou S and Schatz G C 2005 *J. Chem. Phys.* **122** 097102
- [23] Markel V A 1993 *J. Mod. Opt.* **40** 2281
- [24] Markel V A 2005 *J. Chem. Phys.* **122** 097101
- [25] Citrin D S 2005 *Nano Lett.* **5** 985
- [26] Zou S and Schatz G C 2006 unpublished
- [27] Zou S and Schatz G C 2004 *Chem. Phys. Lett.* **403** 62
- [28] Kahl M, Voges E, Kostrewa S, Viets C and Hill W 1998 *Sensors Actuators B* **51** 285
- [29] Hicks E M, Zhang X, Zou S, Lyandres O, Spears K G, Schatz G C and Van Duyne R P 2005 *J. Phys. Chem. B* **109** 22351
- [30] Salerno M, Krenn J R, Hohenau A, Ditlbacher H, Schider G, Leitner A and Aussenegg F R 2005 *Opt. Commun.* **248** 543
- [31] Mackowski D W 1994 *J. Opt. Soc. Am. A* **11** 2851
- [32] Mackowski D W 2001 *J. Quantum Spectrosc. Radiat. Transfer* **70** 441
- [33] Zhao L, Kelly K L and Schatz G C 2003 *J. Phys. Chem. B* **107** 7343
- [34] Hao E and Schatz G C 2004 *J. Chem. Phys.* **120** 357
- [35] Gunnarsson L, Rindzevicius T, Prikulis J, Kasemo B, Kall M, Zou S and Schatz G C 2005 *J. Phys. Chem. B* **109** 1079
- [36] Lynch D W and Hunter W R 1985 *Optical Constants of Metals* ed E D Palik (New York: Academic) p 350